

Fine structure in electronic transitions attributed to nitrogen donor in silicon carbide

Cite as: Appl. Phys. Lett. **119**, 262101 (2021); <https://doi.org/10.1063/5.0074046>

Submitted: 06 October 2021 • Accepted: 14 December 2021 • Published Online: 27 December 2021

N. Assmann,  C. Persson,  A. Yu. Kuznetsov, et al.



View Online



Export Citation



CrossMark

ARTICLES YOU MAY BE INTERESTED IN

[Opportunities for energy level tuning at inorganic/organic semiconductor interfaces](#)

Applied Physics Letters **119**, 260501 (2021); <https://doi.org/10.1063/5.0074963>

[Rhombohedral and turbostratic boron nitride: X-ray diffraction and photoluminescence signatures](#)

Applied Physics Letters **119**, 262102 (2021); <https://doi.org/10.1063/5.0076424>

[Over 1.8 GW/cm² beveled-mesa NiO/ \$\beta\$ -Ga₂O₃ heterojunction diode with 800 V/10 A nanosecond switching capability](#)

Applied Physics Letters **119**, 262103 (2021); <https://doi.org/10.1063/5.0071280>



Timing is everything.
Now it's automatic.

A new synchronous source measure system for electrical measurements of materials and devices

 **Lake Shore**
CRYOTRONICS

[Learn more](#)

Fine structure in electronic transitions attributed to nitrogen donor in silicon carbide

Cite as: Appl. Phys. Lett. **119**, 262101 (2021); doi: [10.1063/5.0074046](https://doi.org/10.1063/5.0074046)

Submitted: 6 October 2021 · Accepted: 14 December 2021 ·

Published Online: 27 December 2021



View Online



Export Citation



CrossMark

N. Assmann,^{1,2} C. Persson,¹  A. Yu. Kuznetsov,¹  and E. V. Monakhov^{1,a)} 

AFFILIATIONS

¹Centre for Materials Science and Nanotechnology, Department of Physics, University of Oslo, Blindern, P.O. Box 1048, 0316 Oslo, Norway

²University of Heidelberg, Im Neuenheimer Feld 225, 69120 Heidelberg, Germany

^{a)} Author to whom correspondence should be addressed: Eduard.Monakhov@fys.uio.no

ABSTRACT

Nitrogen in group-IV semiconductors has become a well-established element of qubits capable of room-temperature operation. In silicon carbide, nitrogen can occupy different nonequivalent lattice sites, giving rise to different shallow donor states. We report a triplet fine structure in electronic transitions of nitrogen donors on the quasi-cubic carbon site in 4H silicon carbide with activation enthalpies of around 100 meV. The intensities of triplet components have a prominent dependence on the voltage bias. The activation enthalpies of the transitions exhibit the Poole–Frenkel effect, while no bias dependence is observed for the magnitude of splitting. A tentative explanation of the fine structure involves local symmetry changes due to stacking faults.

Published under an exclusive license by AIP Publishing. <https://doi.org/10.1063/5.0074046>

Nitrogen has emerged recently as an important building block for qubits in semiconductors. Nitrogen-vacancy (NV) qubits in diamond have given a promise of room-temperature quantum computers.¹ Similar hopes are associated with NV in silicon carbide (SiC),^{2,3} and it is more beneficial than NV in diamond since optical properties are more compatible with fiber optics communication. Notably, the presence of nonequivalent lattice sites in SiC for both nitrogen and vacancies complicates the investigations on the one hand, but on the other hand, may provide additional flexibilities for the qubits design and control.

One of the first detailed spectroscopic studies on ionization energies of nitrogen donors in 4H polytype SiC (4H-SiC) was performed by Götz *et al.*⁴ Infrared (IR) absorption spectroscopy and Hall-effect measurements have revealed the presence of two dominant donor levels with ionization energies of 52.1 and 91.8 meV. The shallower level was assigned to nitrogen on the quasi-hexagonal carbon site, N(h), and the deeper level was assigned to nitrogen on the quasi-cubic carbon site, N(k). The effective mass approximation (EMA), with the extension by Faulkner,⁵ could accurately describe the excitation levels for both donor symmetries. In addition, Götz *et al.*⁴ have observed a valley-orbit (VO) splitting of the ground 1s-state of N(h) to 1s(A₁) and 1s(E) states, exhibiting ~ 7.6 meV splitting. However, a similar VO-splitting foreseeable for the deeper N(k) was not observed, presumably due to limitations of the method.

Chen *et al.*⁶ have improved the energy resolution by almost an order of magnitude using photothermal ionization spectroscopy on a free-standing, moderately doped 4H-SiC epitaxial layer. The ionization energy of the shallow N(h) was deduced to be 60.2 ± 0.5 meV. The energy of the VO-splitting between 1s(A₁) and 1s(E) of N(h) was established to be 7.4 ± 0.1 meV. Later, Ivanov *et al.*⁷ re-visited the data by Chen *et al.*⁶ and deduced the ionization energy of N(h) to be 61.4 ± 0.5 meV. A more recent investigation of the deeper N(k) by the donor–acceptor pair luminescence resulted in an ionization energy of 125.5 meV.⁸ The findings and assignments mentioned above correlate with the trend observed in density functional theory (DFT) calculations,⁹ where the ionization energies for N(h) and N(k) are estimated as 0.081 and 0.261 eV, respectively.

The emergence of high-quality epitaxial 4H-SiC with moderate doping has opened the possibility of studies using junction spectroscopy such as thermal admittance spectroscopy (TAS) and deep level transient spectroscopy (DLTS). Since the pioneering studies by Kimoto *et al.*,¹⁰ the electronic transitions attributed to N(h) and N(k) are routinely observed by these electrical techniques. TAS measurements normally result in the ionization enthalpies in the range 45–65 meV for N(h) and around 100–130 meV for N(k).¹⁰ The application of DLTS to spectroscopic studies of the shallow donors is limited, since DLTS is designed for investigating deep levels, where the freeze out of the shallow donors can be neglected. Nevertheless, the

transition attributed to N(k) can be observed and analyzed in some cases (see, for instance, very recent study by Gelczuk *et al.*¹¹).

As mentioned above, optical spectroscopy of N(h) has resulted in a detailed picture of the electronic states, while the optical measurements of N(k) are challenging. In this study, we have investigated the level assigned in the literature to N(k) by DLTS with improved energy resolution. We have observed a triplet fine structure of this level. The origin of this triplet splitting is discussed in terms of symmetry changes. One of the likely explanations can involve local polytype changes due to stacking faults (SFs) in 4H-SiC.

Samples used in the study were cut from a state-of-the-art, high-quality 6-in. (0001) 4H-SiC wafer commercially purchased from Cree, Inc. The material is a 10- μm thick 4H-SiC epitaxial layer with a nitrogen doping concentration of $1 \times 10^{15} \text{ cm}^{-3}$ grown on the Si-face of a 350- μm n-type 4H-SiC substrate with a 0.5- μm thick 4H-SiC epitaxial buffer layer. Nitrogen doping of the buffer layer and the substrate is in the range 10^{18} and 10^{19} cm^{-3} , respectively. The *c*-axis of the substrate and the epitaxial layers is intentionally 4° off the normal to the surface with a random lateral direction.

For electrical characterization, Schottky diodes were fabricated. The samples were first cleaned by dipping in a 10% HF solution for 10 min followed by rinsing with distilled water. Gold contacts with a 1.2-mm diameter and thicknesses between 280 and 370 nm were then deposited using thermal evaporation at pressures around 10^{-5} – 10^{-4} mbar. Silver paste was used as the backside contact.

TAS measurements were carried out with heating and cooling rates of $\sim 1 \text{ K/min}$ in the temperature range of 20–300 K using an Agilent 4284A LCR meter. Capacitance and conductance were measured at probe frequencies between 100 Hz and 1 MHz with an AC signal of 20 mV.

DLTS spectra were measured with a Boonton 7200 capacitance meter and a closed-cycle helium cryostat. The DLTS signal was deduced from the acquired capacitance transients using the so-called “lock-in” and GS4 weighting functions¹² with time windows in the range 20–640 ms. The heating rate in the DLTS measurements was 0.5–1 K/min. The reverse voltage bias in the range 1–12 V was used with a corresponding filling pulse voltage to probe the full depletion region in the epilayer down to the depth $\sim 5 \mu\text{m}$.

Figure 1(a) depicts typical results of TAS measurements at 10 V reverse voltage in the temperature range 20–300 K, where the capacitance of the Schottky diode is plotted as a function of temperature for different probing frequencies. The spectra are dominated by two step-like drops in the capacitance that correspond to electronic levels with activation enthalpies of 57 and 105 meV. In accordance with literature,^{4–11} we identify these levels as N(h) and N(k). Notably, the drop in capacitance due to the N(k) freeze out is relatively small: from ~ 56 to ~ 52 pF, see Fig. 1(a). We estimated it to correspond to $\sim 15\%$ donor freeze out, which implies that the fractions of N(k) and N(h) are $\sim 15\%$ and $\sim 85\%$, respectively. Such a difference in the population of N(h) and N(k) indicates $\sim 0.1 \text{ eV}$ higher formation energy of N(k), assuming a growth temperature of $\sim 1500^\circ\text{C}$. This is in agreement with DFT calculations by Weber *et al.*,¹³ which indeed predicted a slightly higher formation energy for N(k). Nitrogen incorporation during crystal growth is an interesting research topic by itself, and different reports may provide conflicting results (see, for instance, Ref. 14 and references therein). It will not, however, be the focus of this study.

A closer look into the N(h) freeze out at $\sim 30 \text{ K}$ in Fig. 1(a) reveals two overlapping shoulders, most pronouncedly resolved for 350 Hz and 1 kHz data. Such behavior can, in fact, be expected. It is in accordance with the VO-splitting (7–8 meV) for the 1s ground state of N(h) established previously by Götz *et al.*⁴ and Chen *et al.*⁶ TAS measurements, however, do not have sufficient energy resolution to characterize this VO-splitting in detail.

Complementary to the TAS data in Fig. 1(a), the DLTS spectra are shown in Fig. 1(b). The DLTS signal is plotted as $2\Delta C/C_r$, where ΔC is the amplitude of the transient and C_r is the steady-state capacitance at the reverse voltage. In an idealized case of uniform concentrations, this expression is equal to the ratio of the electron trap concentration, N_t , to the donor concentration, N_d :¹⁵ $2\Delta C/C_r = N_t/N_d$. The spectra reveal two DLTS peaks at around 50 and 300 K. The most dominant peak occurs at around 50 K. It has an amplitude that corresponds to about 15% of doping and is consistent with that of N(k), as observed with TAS in Fig. 1(a). Careful examination of the N(k) peak has revealed an indication of a fine structure, which will be the matter of detailed investigation in the rest of this text. It should be pointed out that the shallower N(h) cannot be observed with DLTS since the

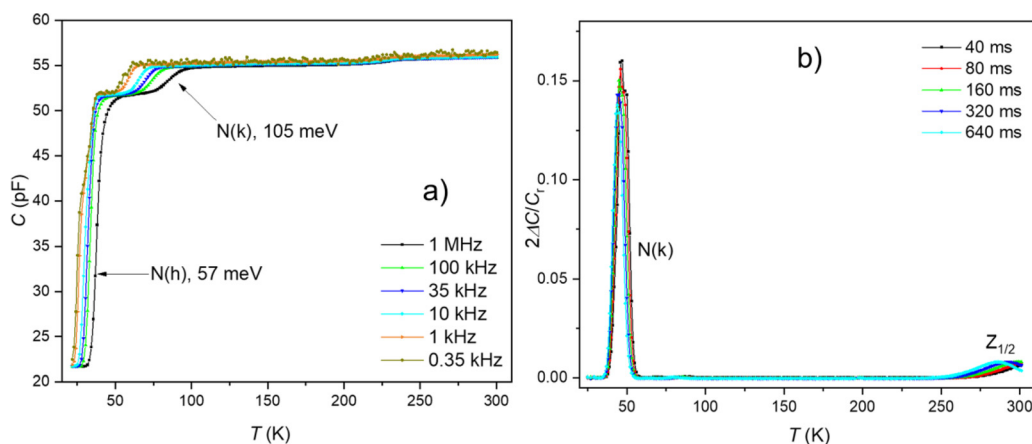


FIG. 1. (a) Capacitance at a reverse voltage of 10 V as a function of temperature for different frequencies. (b) DLTS spectra measured at 10 V reverse voltage for different time windows and employing the “lock-in” weighting function.

freeze out of $N(h)$ results in complete carrier freeze out. The DLTS peak at around 300 K is normally labeled as $Z_{1/2}$ in the literature, and it is assigned to two overlapping levels of carbon vacancies at h- and k-sites (see Refs. 11 and 16 and references therein).

High-resolution DLTS spectra for the $N(k)$ peak measured in the temperature range 35–55 K for different time windows are shown in Fig. 2(a). The increased resolution was obtained by performing the measurements with a temperature step of 0.5 K and employing the GS4 weighting function.¹² Similar to the results in Fig. 1, the measurements were performed at a reverse voltage of 10 V. We observe that the $N(k)$ peak exhibits a triplet fine structure previously not reported in the literature, and we label the components as $N(k)_{-1}$, $N(k)_0$, and $N(k)_{+1}$. The analysis of the activation enthalpies is performed using the Arrhenius plot [Fig. 2(b)] for emission rates, e_n , in accordance with the approach developed by Lang.¹⁵ It results in the activation enthalpies 101 ± 3 , 119 ± 2 , and 126 ± 2 meV for $N(k)_{-1}$, $N(k)_0$, and $N(k)_{+1}$, respectively.

It should be noted that the concentration of $N(k)$, which amounts to $\sim 15\%$ of the total doping concentration, is at the limit of the DLTS applicability. In the case of high concentrations, the capacitance transients are not strictly exponential. This unfortunately rules out the application of Laplace DLTS¹⁷ that has potentially higher energy resolution by relying on the exponential shape of the transient. However, the conventional approach, which uses a weighting function for transient analysis, can be applied. We have shown previously¹⁸ that nonexponential transients, due to very high local concentrations of emission centers, will affect the shape of the DLTS peak. Both the amplitude and the peak positions will be perturbed, but it will not result in the appearance of satellite peaks and/or a fine structure. In addition, the observed fine structure is present for all the time windows; and the DLTS peaks in Fig. 2 exhibit different positions for different time windows in accordance with the Arrhenius behavior of the corresponding emission rates. We can conclude that the observed fine structure is indeed a newly observed physical phenomenon and not a methodological artifact.

Measurements at different applied voltages have revealed the following dependencies for $N(k)_{-1}$, $N(k)_0$, and $N(k)_{+1}$ [Figs. 3(a) and 3(b)]

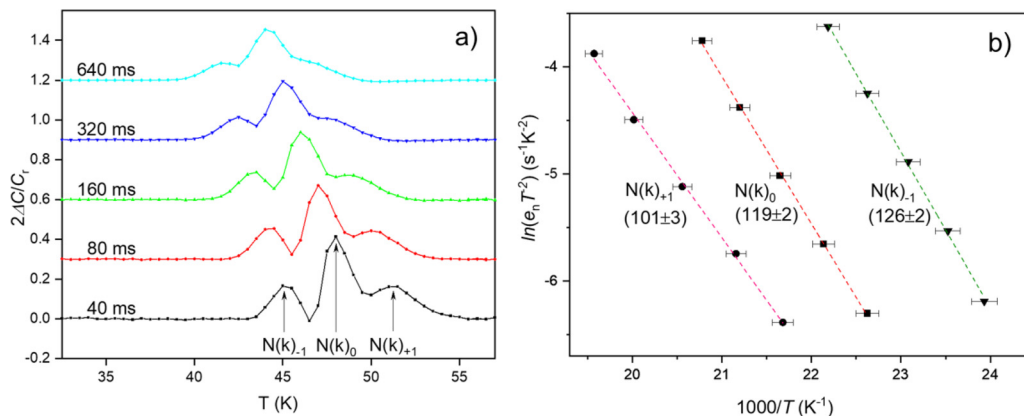


FIG. 2. (a) High-resolution DLTS spectra recorded at 10 V reverse voltage with a temperature step of 0.5 K for different time windows and by employing the GS4 weighting function. (b) Arrhenius plot for the emission rates of $N(k)_{-1}$, $N(k)_0$, and $N(k)_{+1}$ peaks.

- (1) The amplitudes of $N(k)_{-1}$, $N(k)_0$, and $N(k)_{+1}$ exhibit a significant dependence on the voltage [Fig. 3(a)]. Indeed, the amplitudes of $N(k)_{-1}$ and $N(k)_{+1}$ at lower voltages are significantly weaker as compared to the amplitude of the central peak $N(k)_0$. As the voltage increases, the amplitudes of $N(k)_{-1}$ and $N(k)_{+1}$ increase at the expense of the central $N(k)_0$.
- (2) The magnitude of splitting among $N(k)_{-1}$, $N(k)_0$, and $N(k)_{+1}$ does not appear to depend on the voltage. Each measurement at different voltages represents an individual temperature scan, and some thermal drift (≤ 1 K) between the measurements cannot be excluded. However, the relative separation $N(k)_{-1}$ -to- $N(k)_0$ and $N(k)_0$ -to- $N(k)_{+1}$ remains constant, ~ 3 K, within the experimental accuracy [Fig. 3(b)].
- (3) All triplet components exhibit the Poole-Frenkel effect, i.e., the activation enthalpies decrease with increasing electric field, which is manifested by the shift of the peaks toward lower temperatures. This is the characteristic of shallow donor centers and consistent with the identification of $N(k)$.

Thus, as it is already interpreted based on the data in Fig. 2, the $N(k)$ triplet is systematic and confirmed in Fig. 3. Moreover, the $N(k)$ fine structure behavior as a function of voltage is spectacular, potentially providing opportunities to control the occupancy of different triplet components by an electric field. At this point, without claiming fully consistent explanation, we can suggest the following tentative explanations.

As mentioned in the introduction, VO-splitting for $N(h)$ as deduced from optical measurements is ~ 7 meV.^{4,6} A similar VO-splitting is expected also for $N(k)$, although it could not be observed experimentally.⁴ Due to the absence of experimental data, we cannot completely rule out the possibility of a triplet VO-splitting for $N(k)$.

Another possible and perhaps more likely explanation can involve stacking faults (SFs) along the c-axis, which break the stacking symmetry of 4H-SiC. It is well-known that SFs in the hexagonal 4H-SiC matrix can result in layers of 3C polytype, forming cubic SiC regions of variable thicknesses embedded in 4H-SiC (see Ref. 19 and references therein). This effectively forms a heterostructure of 4H- and 3C-SiC and a corresponding quantum well. 8H-like heterostructures have also been reported.²⁰ The presence of locally altered stacking

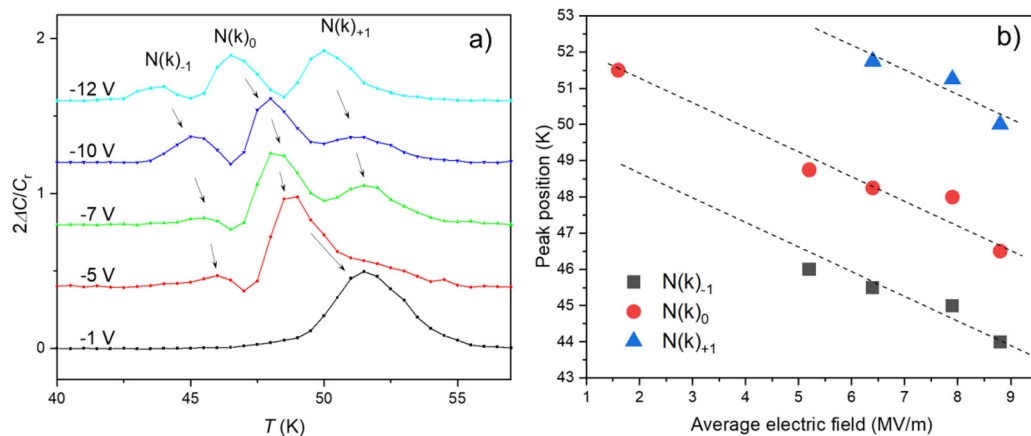


FIG. 3. (a) High-resolution DLTS spectra recorded at different reverse voltages for the time window 40 ms and by employing the GS4 weighting function. The arrows show the shifts of the peaks for different voltages. (b) Peak positions in the DLTS spectra vs the average electric field in the depletion region. The dashed lines are for guiding the eye and to indicate the trend. The average electric field is calculated as the applied voltage divided by the depletion region width.

symmetry and, thus, a quantum well in the vicinity of the nitrogen atom will affect the ionization energy. This may result in several discrete values depending on the symmetry type of SFs. Interestingly, Ivády *et al.*²¹ have reported recently on stabilization of point-defect spin qubits utilizing the effect of SFs on the local stacking symmetry in 4H-SiC. They were able to identify previously unattributed room-temperature qubits (known as PL5–7 defect qubits in the literature^{2,22}) as divacancies in SFs-induced quantum wells. Thus, potentially, the $N(k)$ triplet could be correlated with the SFs. Within this scenario, the effect of the applied bias on the intensities of the triplet implies nonhomogeneous distribution of the SFs in accordance with the different depths probed at different voltages in Fig. 3(a), which is unlikely in modern high quality epi-wafers. On the other hand, the effect may be due to the electric field that affects quantum well barriers, rather than the probing depth.

One can argue that in the latter case, the amount and the character of SFs can vary from wafer to wafer depending on the growth conditions. We have performed DLTS measurements on a different wafer from a different fabrication batch (see details in the [supplementary material](#)). We can confirm the presence of a fine structure for $N(k)$ also in the other wafer. However, this fine structure has a significantly different shape with two dominant transitions. Due to the sensitivity of the method, the presence of the third transition could not be conclusively confirmed or ruled out. We interpret this deviation between different wafers as supporting the stacking fault hypothesis.

In conclusion, DLTS analysis of the electronic transition associated with $N(k)$ in 4H-SiC reveals a triplet fine structure. The components of the fine structure exhibit the Poole–Frenkel effect, as expected for shallow donors. The amplitudes of the components display prominent dependence on the applied voltage. In contrast, the splitting between the components shows no voltage dependence. A tentative explanation of the observations involves symmetry changes due to SFs.

See the [supplementary material](#) for description of DLTS analysis with the so-called GS4 weighting function and the details and results of DLTS measurements on a different wafer from a different fabrication batch.

We would like to thank Professor A. Winnacker for his useful comments. We acknowledge Research Council of Norway for support via the Norwegian Micro- and Nano-Fabrication Facility, NorFab (Project No. 245963).

AUTHOR DECLARATIONS

Conflict of Interest

The authors have no conflicts to disclose.

DATA AVAILABILITY

The data that support the findings of this study are available from the corresponding author upon reasonable request.

REFERENCES

- ¹R. Hanson and D. D. Awschalom, *Nature* **453**, 1043 (2008).
- ²W. F. Koehl, B. B. Buckley, F. J. Heremans, G. Calusine, and D. D. Awschalom, *Nature* **479**, 84 (2011).
- ³A. Csöré, H. J. von Bardeleben, J. L. Cantin, and A. Gali, *Phys. Rev. B* **96**, 085204 (2017).
- ⁴W. Götz, A. Schöner, G. Pensl, W. Suttrop, W. J. Choyke, R. Stein, and S. Leibenzeder, *J. Appl. Phys.* **73**, 3332 (1993).
- ⁵R. A. Faulkner, *Phys. Rev.* **184**, 713 (1969).
- ⁶C. Q. Chen, J. Zeman, F. Engelbrecht, C. Peppermüller, R. Helbig, Z. H. Chen, and G. Martinez, *J. Appl. Phys.* **87**, 3800 (2000).
- ⁷I. G. Ivanov, B. Magnusson, and E. Janzén, *Phys. Rev. B* **67**, 165212 (2003).
- ⁸I. G. Ivanov, A. Henry, and E. Janzén, *Phys. Rev. B* **71**, 241201(R) (2005).
- ⁹M. Miyata, Y. Higashiguchi, and Y. Hayafuji, *J. Appl. Phys.* **104**, 123702 (2008).
- ¹⁰T. Kimoto, A. Itoh, H. Matsunami, S. Sridhara, L. L. Clemen, R. P. Devaty, W. J. Choyke, T. Dalibor, C. Peppermüller, and G. Pensl, *Appl. Phys. Lett.* **67**, 2833 (1995).
- ¹¹Ł. Gelczuk, M. Dąbrowska-Szata, V. Kolkovsky, M. Sochacki, J. Szmidi, and T. Gotszalk, *J. Appl. Phys.* **127**, 064503 (2020).
- ¹²A. A. Istratov, *J. Appl. Phys.* **82**, 2965 (1997).
- ¹³J. R. Weber, W. F. Koehl, J. B. Varley, A. Janotti, B. B. Buckley, C. G. van de Walle, and D. D. Awschalom, *J. Appl. Phys.* **109**, 102417 (2011).
- ¹⁴G. Ferro and D. Chaussende, *Sci. Rep.* **7**, 43069 (2017).
- ¹⁵D. V. Lang, *J. Appl. Phys.* **45**, 3023 (1974).
- ¹⁶H. M. Ayyedh, R. Nipoti, A. Hallén, and B. G. Svensson, *J. Appl. Phys.* **122**, 025701 (2017).
- ¹⁷L. Dobaczewski, P. Kaczor, I. D. Hawkins, and A. R. Peaker, *J. Appl. Phys.* **76**, 194 (1994).

- ¹⁸E. V. Monakhov, J. Wong-Leung, A. Yu. Kuznetsov, C. Jagadish, and B. G. Svensson, *Phys. Rev. B* **65**, 245201 (2002).
- ¹⁹R. Hristu, S. G. Stanciu, D. E. Tranca, E. K. Polychroniadis, and G. A. Stanciu, *Sci. Rep.* **7**, 4870 (2017).
- ²⁰H. Fujiwara, T. Kimoto, T. Tojo, and H. Matsunami, *Appl. Phys. Lett.* **87**, 051912 (2005).
- ²¹V. Ivády, J. Davidsson, N. Deegan, A. L. Falk, P. V. Klimov, S. J. Whiteley, S. O. Hruszkewycz, M. V. Holt, F. J. Heremans, N. T. Son, D. D. Awschalom, I. A. Abrikosov, and A. Gali, *Nat. Commun.* **10**, 5607 (2019).
- ²²A. L. Falk, B. B. Buckley, G. Calusine, W. F. Koehl, V. V. Dobrovitski, A. Politi, C. A. Zorman, P. X.-L. Feng, and D. D. Awschalo, *Nat. Commun.* **4**, 1819 (2013).